View metadata, citation and similar papers at core.ac.uk

brought to you by CORE

provided by Elsevier - Publisher Connector

Journal of Taibah University for Science 9 (2015) 579–585

www.elsevier.com/locate/jtusci

Naphthalimide-derivative with blue electroluminescence for OLED applications☆

E.R. Triboni [a], M.R. Fernandes [b], J.R. Garcia [c], M. Costa Carreira [b], R.G.S. Berlinck [b], P. Berci Filho [b], L.S. Roman [d], I.A. Hümmelgen [d], R. Reyes [e,*], M. Cremona [f,g]

[a] *Departamento de Engenharia Química, EEL Universidade de São Paulo, São Paulo, SP, CEP 12602-810, Brazil*
[b] *Instituto de Química de São Carlos, Universidade de São Paulo, C.P. 780, São Carlos, SP, CEP 13560-970, Brazil*
[c] *Departamento de Química, Universidade Estadual de Ponta Grossa, Ponta Grossa, PR, CEP 84030-900, Brazil*
[d] *Departamento de Física, Universidade Federal do Paraná, C.P. 19044, Curitiba, PR, CEP 81531-990, Brazil*
[e] *Facultad de Ingenieria Quimica y Textil, Universidad Nacional de Ingenieria, Av. Tupac Amaru 210, Lima 31, Peru*
[f] *DIMAT – Divisão de Metrologia de Materiais, Instituto Nacional de Metrologia, Normalização e Qualidade Industrial, INMETRO, Duque de Caxias, RJ, Brazil*
[g] *Departamento de Física, Pontifícia Universidade Católica do Rio de Janeiro, PUC-Rio, C. P. 38071, Rio de Janeiro, RJ, CEP 22453-970, Brazil*

Available online 6 April 2015

Abstract

The synthesis and characterization of the 4-(2-fenoxi-p-xileno)-N-methyl-1,8-naphthalimide, referred to here as NPOX, is described in this work. The characterization of NPOX was performed using proton nuclear magnetic resonance spectroscopy (^{1}H NMR), UV–visible and fluorescence emission spectroscopy. The LUMO and HOMO levels of NPOX were estimated using the electrochemical method, respectively, at 3.4 eV and 6.1 eV with an energy gap of 2.7 eV. The NPOX is soluble in chloroform such that when it evaporates, it becomes a transparent film with fluorescence emissions occurring at 456 nm when excited at 363 nm. Using the Space-Charge-Limited-Current (SCLC) model, we obtained the value of the mobility of the positive charge carriers to be $\mu \cong 5 \times 10^{-5}$ cm^2 V^{-1} s^{-1}. These properties raise the possibility of using the NPOX as the emitting layer in an organic light-emitting diode (OLED) with emission in the blue region, as demonstrated by the fabrication of an OLED with an ITO/PEDOT:PSS/NPOX/Al structure and light emission peaking at approximately 465 nm.
© 2015 The Authors. Production and hosting by Elsevier B.V. on behalf of Taibah University. This is an open access article under the CC BY-NC-ND license (http://creativecommons.org/licenses/by-nc-nd/4.0/).

Keywords: Naphthalimide; Organic diode; Fluorescence; Electroluminescence; OLED

1. Introduction

Organic electroluminescent (EL) devices are of great interest because of their efficient emissions in the visible region and their potential applications in full colour large-area flat panel displays. Electroluminescence in polymeric or molecular materials is obtained by the recombination of electrons and holes injected at the anode and cathode, respectively. Much effort has been put into the development of new organic EL molecular materials and appropriate device structures to achieve high-efficiency and stable devices with defined emission colours. Of the various kinds of EL materials, 1,8-naphthalimide derivatives have attracted attention due to their high photoluminescence quantum yields

☆ Peer review under responsibility of Taibah University

* Corresponding author. Tel.: +51 14817919.
E-mail address: fisicaplic@hotmail.com (R. Reyes).

Production and hosting by Elsevier

http://dx.doi.org/10.1016/j.jtusci.2015.03.013
1658-3655 © 2015 The Authors. Production and hosting by Elsevier B.V. on behalf of Taibah University. This is an open access article under the CC BY-NC-ND license (http://creativecommons.org/licenses/by-nc-nd/4.0/).

and good optical, thermal and chemical stabilities [1–3]. The 1,8-Naphthalimide derivatives have unique photophysical properties, which have been widely used as brilliant yellow dyes in synthetic fiber technology, as functional segments for the design of dual-mode chemical (protons)/electrochromic molecular switches and as functional fluorescent imaging polymers [4–6].

With the use of organic materials, there is a possibility of obtaining many different colours within the fluorescence emissions [7]. In the case of naphthalimides, variations in the colours may be obtained by changes in the donor group in position 4 of the naphthalene moiety [4,8,9]. In our research, we have determined that the coupling between the 4-nitro-N-methyl-1,8-naphthalimide and 2-hydroxi-p-xylen produces an organic material 4-(o-oxi-p-xylen)-N-methyl-1,8-naphthalimide, which has the capacity to form films capable of blue light emissions. It is important to note that this molecule, referred to here as NPOX, is different from other naphthalimide derivatives capable of blue light emissions [10–12] because it has an aromatic replacement in position 4 of the naphthalene moiety that is coupled by an ether ligand.

In this work, we present the synthesis and characterization of the naphthalimide-derivative NPOX. We also demonstrate that this organic molecule can be used to fabricate an organic light-emitting diode (OLED) with emissions in the blue light region.

2. Materials and methods

According to a previously described procedure [13,14], the 4-nitro-N-methyl-1,8-naphthalimide was synthesized through the reaction of 4-nytro-1,8-anhydrid-naphthalic with methyl amine via ultrasonification in water for 1 h with a reaction yield of 90%. This compound was reacted with 2-hydroxi-p-xylen sodium salt in acetonitrile and a small amount of K_2CO_3 while stirred at 40 °C for 8 h to yield the 4-(o-oxi-p-xylen)-N-methyl-1,8-naphthalimide (NPOX). The time at which the reaction ceased was determined by thin-layer chromatography (TLC). The solvent was then vacuum evaporated and the crude product was extracted with CH_2Cl_2 and washed first with a 5% NaOH solution and then with water. The organic phase was separated and dried with $MgSO_4$. The NPOX reaction yield was 95%. The melting point was 169 °C and the re-crystallization of this product in ethanol produced yellow crystals consisting of a needle-like shape.

NPOX films were obtained using a spin-coating technique from the solution containing $CHCl_3$ (10 mg/ml). The film thickness was determined using a Dektak3 surface profiler.

Using $CHCl_3$ as a solvent and tetramethylsilane as an internal reference, the NPOX was characterized via proton nuclear magnetic resonance (^{1}H NMR) in a Brukker AC200 spectrometer. Gas chromatography and mass spectrometry (GC/MS) analysis were performed on a HP-5890 mass spectrometer and the infrared (IR) spectrum of the NPOX film deposited on the silicon substrate was recorded using a Bomen-MB 102 spectrometer.

The ultraviolet–visible (UV–vis) absorption analysis of the NPOX film deposited on the silicon substrate was performed using a Varian-Cary 5G spectrophotometer. The fluorescence spectra were determined using a diluted solution and from a thin film on a quartz substrate using a Hitachi F4500 spectrophotometer.

Cyclic voltammetry (CV) measurements were carried out on a FAC-potentiostat and the HOMO and LUMO levels of the NPOX were estimated by determining the onset of the electrochemical oxidation and reduction of the organic film, respectively, in an acetonitrile solution of 0.1 mol L^{-1} of $LiClO_4$. Each solution potential was determined from different experiments to avoid the interference of the irreversibilities associated with the film oxidation. Details of the method used here are described by Micaroni et al. [15].

To investigate the possibility of using NPOX as the emitting layer in OLEDs, samples were fabricated using Indium-Tin oxide (ITO) covered with (Poly(3,4-ethylenedioxythiophene)) – Poly(styrene sulfonate), PEDOT:PSS, which was supplied by Bayer AG and Al as the electrode in the ITO/PEDOT:PSS/NPOX/Al architecture. The NPOX film was deposited by spin coating from a chloroform solution (10 mg/ml) and the Al electrode was evaporated [16], on top of the NPOX layer through a shadow mask to limit the active area of the device to ∼2 mm^2.

The current and voltage characteristics were recorded with a Keithley voltage source and recorded in a nitrogen atmosphere. The electroluminescence spectra of the OLEDs were obtained in a Photon Technology International (PTI) fluorescence spectrophotometer and the brightness was measured using a calibrated radiometer/photometer from United Detector Technology (UDT-350).

3. Results and discussion

3.1. Chemical characterization of the NPOX compound

For the sake of clarity, the structural formula of the product is given in Fig. 1. Following the description in Fig. 1, the ^{1}H NMR spectrum (Fig. 2) chemical shifts (δ)

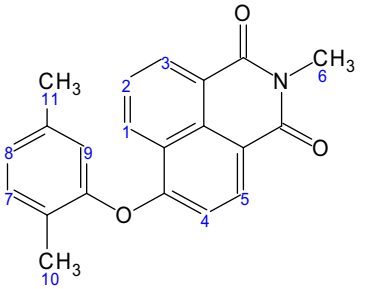

Fig. 1. Structural formula of the NPOX.

that were observed are: ^{1}H NMR (200 MHz, CDCl3) δ 2.06 (s, 3H, CH3), 2.28 (s, 3H, CH3), 3.47 (s, 3H, CH3), 6.63 (d, 1H, CH), 6.86 (s, 1H, CH), 6.98 (d, 1H, CH), 7.16 (d, 1H, CH), 7.72 (t, 1H, CH), 8.35 (d, 1H, CH), 8.60 (d, 1H, CH) and 8.67 (d, 1H, CH), where s, d and t stand for singlet, doublet and triplet bands, respectively. Using this spectrum, the NMR can be verified so that the obtained product has a high purity. The three singlet bands, which are assigned to the methyl groups, yielded an integrated intensity of 3, whereas the other eight signals, which are assigned to the aromatic protons, give integrated intensities of 1, which is coherent with the structure described in Fig. 1.

The GC/MS analysis produced a single peak in the chromatogram (not shown here), revealing a highly pure product. The mass spectrum showed $m/z = 331$ (molecular ion), $m/z = 120$ (fenoxi fragment) and $m/z = 211$ (N-phthalimide fragment). The strongest peak is from the most abundant molecular ion due to its high stability, which is the result of the presence of the two aromatic rings that facilitate its ionization.

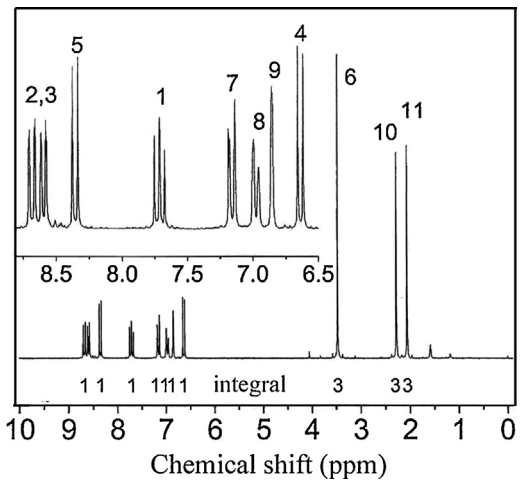

Fig. 2. NPOX nuclear magnetic resonance of proton (^{1}H NMR) spectrum with $CHCl_3$ as solvent and tetramethylsilane as internal reference.

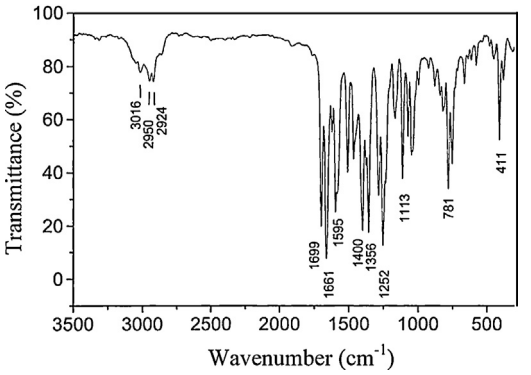

Fig. 3. Infrared spectrum of the NPOX film deposited on silicon substrate.

The IR spectrum of the compound (Fig. 3) exhibits a pair of peaks at the 1699 cm^{-1} and 1661 cm^{-1} bands due to the asymmetric and symmetric carbonyl stretching, respectively, and the 1356 cm^{-1} band due to the C–N–C stretching. The p-xilene bands occurred at 1508 cm^{-1}, due to ring C=C stretching, and at 1041 cm^{-1} and 794 cm^{-1} due to the out of plane and in plane C–H bending. Formation of the C–O–C bonding, which is the bonding between the naphtalimide and p-xilene, was confirmed by the asymmetric and symmetric stretching at 1253 cm^{-1} and 1074 cm^{-1}, respectively [9,17,18].

3.2. Optical and fluorescence studies

The UV–vis absorption spectrum of the NPOX film deposited on the silicon substrate is shown in Fig. 4 (curve a). Three transitions are seen in the spectrum, but only two bands are discernible due to the detection limitations of the UV light. The lowest transition

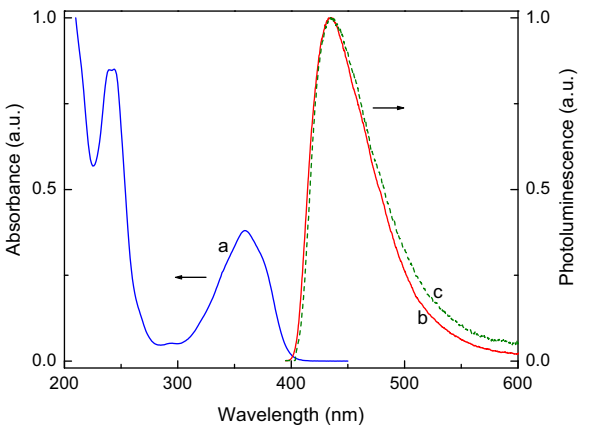

Fig. 4. (a) UV–vis absorption spectrum of NPOX film on a quartz plate, (b) fluorescence spectrum of NPOX in $CHCl_3$ solution (6 mg/ml), (c) fluorescence spectrum of a NPOX film produced by spin-coating from a solution in $CHCl_3$.

peaks at 360 nm and exhibits two additional shoulders at 340 nm and 380 nm. The higher energy transition peaks at 243 nm and exhibits a shoulder at 211 nm. The UV–vis absorption spectrum of the un-substituted 1,8 naphthalimide has been studied by Gawronski et al. [19], and exhibited the lowest state with three bands, which peaked at 355 nm, 320 nm and 315 nm. The higher energy transitions peaked at 225 nm and 211 nm. Compared to the un-substituted 1,8-naphthalimide, all the electronic transitions of the NPOX are red shifted. The red shift is due to changes in the polarisation along the short axis of the naphtalene moiety caused by the substituent at position 4. All the bands of the 1,8-nahpthalimide are assigned to $\pi \rightarrow \pi^*$ transitions between the ground state S_0 and the different excited states [19]. The onset of absorption (400 nm) is taken as the HOMO-LUMO transition of the film with negligible phonon coupling and the energy gap measured at this point is 3.1 eV.

The fluorescence spectrum of the NPOX in the $CHCl_3$ solution and the fluorescence spectrum of a NPOX film are shown in Fig. 4 (curves b and c), respectively. The emission spectra of both the solution and film show a broad peak centred at 435 nm with a marked tail in the lower energy portion of the emission spectra. The structure observed in the absorption spectrum at the band centred at 360 nm is almost lost in the emission spectra. However, the peak shapes are quite similar and result from different transitions at very close energies. Additionally, the emission curve of the NPOX film (curve c) presents only small shifts compared to the emission of the NPOX taken from the solution (curve b), indicating the primarily amorphous character of the deposited film [2,4,12,20]. We also see that the onset of the (0,0) transition in the emission spectra is essentially the same as the (0,0) transition in the absorption spectrum at 400 nm.

3.3. Electrochemical studies

The cyclic voltammogram of the NPOX is presented in Fig. 5. The reduction and oxidation processes were measured separately. The reduction process (curve a) exhibits two waves: one cathodic and one anodic, which reveal that the process is almost reversible. The oxidation process (curve b) presents only one anodic wave, indicating that the film oxidation process is irreversible. The irreversibility implies that the charge transfer may cause chemical changes in the molecular film and that the measured potential is a mix of ionization potential and the energy required for the possible chemical changes occurring during the charge transfer. However, if just the onset potential is examined, the contribution of the chemical changes may be small enough to be ignored.

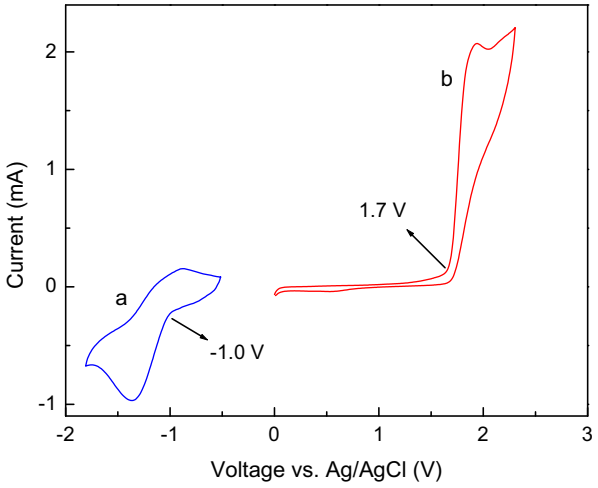

Fig. 5. Cyclic voltammogram of an NPOX film. Oxidation and reduction onsets are indicated.

Examining the onsets of oxidation and reduction, the LUMO and HOMO levels of the NPOX are estimated at 3.4 eV and 6.1 eV, respectively, with an energy gap of 2.7 eV. This energy gap is comparable to that obtained from optical measurements (Fig. 4), which is 3.1 eV if the onset of absorption is used. Since the HOMO value is more reliable, it may be concluded that the LUMO must be between 3.4 eV and 3.0 eV.

3.4. Electrical studies

The $J-V$ characteristic of an ITO/PEDOT:PSS-(60 nm)/NPOX(170 nm)/Al(120 nm) device with a positively biased ITO is presented in Fig. 6. The inset shows

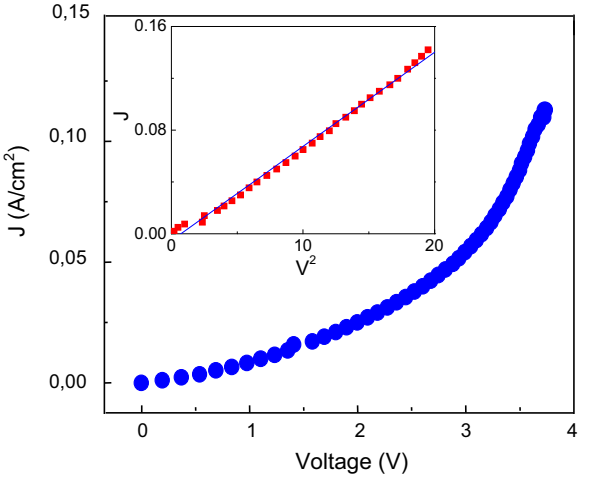

Fig. 6. $J(V)$ characteristics of an ITO/PEDOT:PSS(60 nm)/NPOX (170 nm)/Al(120 nm) device for ITO positively biased. Inset: $I(V^2)$ characteristics of the same device.

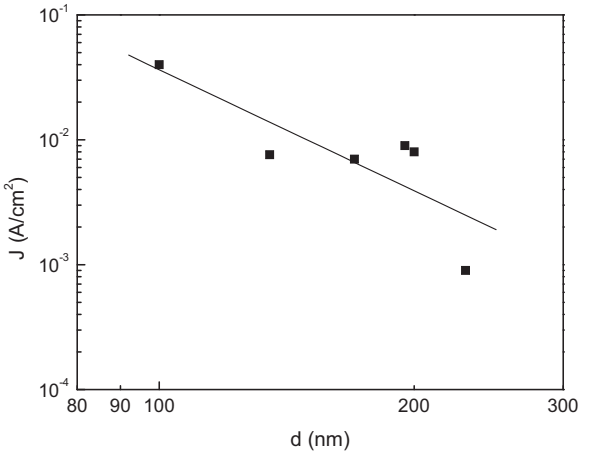

Fig. 7. $J(d)$ characteristics of ITO/PEDOT:PSS(60 nm)/NPOX (d)/Al(120 nm) devices with different NPOX thickness d: 100, 135, 170, 230, 195 and 200 nm. The J values were taken at $V = 1$ V, with ITO positively biased.

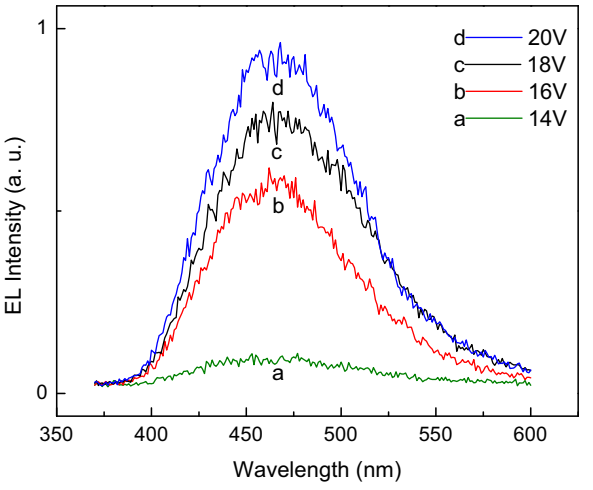

Fig. 8. EL spectrum of a ITO/PEDOT:PSS-(60 nm)/NPOX-(100 nm)/Al(120 nm) OLED device for different voltage values with ITO positively biased.

the $J - V^2$ plot. The linear behaviour in this $J - V^2$ plot suggests that the current is bulk limited. Bulk limited current or Space-Charge-Limited-Current (SCLC) may provide information on the transport of the charge carriers inside the organic layer, allowing the extraction of their mobility [21–23]. In the SCLC model, the current density dependence on the voltage is given by [24]:

$$J = \frac{9\mu\varepsilon V^2}{8d^3}, \tag{1}$$

where ε is the permittivity of the material and μ is the mobility. In this case, the mobility is independent of the applied electric field and the current density. In this regime, the current is expected to depend quadratically on the applied voltage, as shown in the inset of Fig. 6. The J dependence on the thickness d at a fixed voltage of $V = 1$ V measured from samples of different NPOX thicknesses is depicted in Fig. 7. The derivative $\partial \ln J/\partial \ln d \cong -3$ confirms that the SCLC model correctly describes the charge transport. Using Eq. (1) and the $J - V$ characteristics, the mobility of the positive charge carriers in the NPOX was determined to be $\mu \cong 5 \times 10^{-5}\,\mathrm{cm^2\,V^{-1}\,s^{-1}}$. The mobility in the NPOX is found to be independent of the applied field.

This independence of the mobility on the electric field was also observed in Tris(8-hydroxyquiniline)Al, Alq_3, when the samples were prepared under ultra-high vacuum conditions, as described by Kiy et al. [25]. Therefore, in Alq_3, deviations from $J \sim V^2$ were attributed to the presence of impurities. The absence of such deviations in our NPOX samples suggest that the NPOX films have low impurity concentrations, assuming the validity of these results in our NPOX as well.

3.5. Electroluminescence studies

The electroluminescence spectra of OLED with the ITO/PEDOT:PSS(60 nm)/NPOX(100 nm)/Al(120 nm) architecture for different voltages with a positively biased ITO is shown in Fig. 8, with EL peaks centred about 465 nm. At 20 V, the (x, y) chromaticity coordinates of the Commission Internationale de l'Eclairages (CIE) are (0.211, 0.313), which is in the blue region. Finally, Fig. 9 shows the current density and the EL intensity as a function of the voltage applied to the OLED device. It is interesting to observe that up to

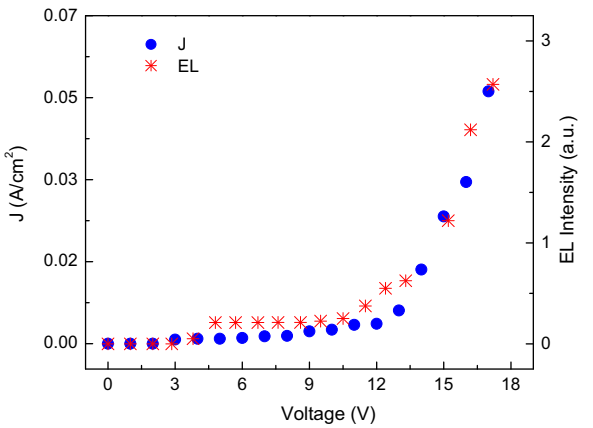

Fig. 9. EL intensity and current density of a ITO/PEDOT:PSS-(60 nm)/NPOX(100 nm)/Al(120 nm) OLED device as a function of applied voltage with ITO positively biased.

17 V, the $J-V$-curve and the EL-intensity-curve have nearly the same shape, suggesting a balanced injection and an approximately constant radiative recombination rate [26].

4. Conclusions

By incorporating an aromatic replacement in position 4 of the naphthalene moiety coupled by an ether ligand, an NPOX compound that is blue light-emitting has been prepared in this work. The synthesis of the NPOX was realised over two phases by reactions producing high yields and products of high purity, which was confirmed using NMR and CG/MS. The solution of NPOX in chloroform formed a film after solvent evaporation, which exhibited blue photoluminescence as a result of the presence of the naphtalimide group. The film forming properties, their photoluminescence and electric behaviour were used to fabricate an OLED with electroluminescence in the blue region. Further investigations are in progress to improve upon these studies and the applications of NPOX in OLEDs.

Acknowledgments

We gratefully acknowledge the contribution of the late Dr. Francisco C. Nart (IQSC-USP) to this work. Also, the authors would like to thank Prof. Sonia R.W. Louro (PUC-Rio) for the use of the spectrofluorimeter and to CNPq, RENAMI, FAPERJ and FAPESP for their financial support. The authors would also like to thank IGI-UNI.

References

[1] Y. Wang, J. Zhou, X. Wang, X. Zheng, Z. Lu, W. Zhang, An efficient guest/host fluorescent energy transfer pair based on the naphthalimide skeleton, and its application in heavily-doped red organic light-emitting diodes, Dyes Pigments 100 (2014) 87–96.

[2] J.A. Mikroyannidis, S. Yeb, Y. Liu, Electroluminesent divinylene- and trivinylene-molecules with terminal naphthalimide or phthalimide segments, Synth. Met. 159 (2009) 492–500.

[3] V. Bojinov, A.I. Venkova, N.I. Georgiev, Synthesis and energy-transfer properties of fluorescence sensing bichromophoric system based on Rhodamine 6G and 1,8-naphthalimide, Sens. Actuators B: Chem. 143 (2009) 42–49.

[4] J. Gan, Q.L. Song, X.Y. Hou, K. Chen, H. Tian, 1,8-Naphthalimides for non-doping OLEDs: the tunable emission color from blue, green to red, J. Photochem. Photobiol. A: Chem. 162 (2004) 399–406.

[5] V. Bojinov, T. Konstantinova, Synthesis of polymerizable 1,8-naphthalimide dyes containing hindered amine fragment, Dyes Pigments 54 (2002) 239–245.

[6] V.B. Bojinov, N.I. Georgiev, P.S. Nikolov, Synthesis and photophysical properties of fluorescence sensing ester- and amidoamine-functionalized 1,8-naphthalimides, J. Photochem. Photobiol. A: Chem. 193 (2008) 129–138.

[7] H. Uoyama, K. Goushi, K. Shizu, H. Nomura, C. Adachi, Highly efficient organic light-emitting diodes from delayed fluorescence, Nature 492 (2012) 234–238.

[8] I. Karamancheva, A. Tadjer, T. Philipova, G. Mandjarova, C. Ivanova, T. Grozeva, Calculated and experimental spectra of some 1,8-naphthalimide derivatives, Dyes Pigments 36 (1998) 273–285.

[9] I. Grabchev, C. Petkov, V. Bojinov, 1,8-Naphthalimides as blue emitting fluorophores for polymer materials, Macromol. Mater. Eng. 287 (2002) 904–908.

[10] C. Adachi, T. Tsutsui, S. Saito, Blue light-emitting organic electroluminescent devices, Appl. Phys. Lett. 56 (1990) 799–801.

[11] S. Yin, X. Liu, C. Li, H. Huang, W. Li, B. He, Electroluminescent properties of naphthalimide derivative thin film devices, Thin Solid Films 325 (1998) 268–270.

[12] Y. Wang, X. Zhang, B. Han, J. Peng, S. Hou, X. Huang, H. Sun, M. Xie, Z. Lu, The synthesis and photoluminescence characteristics of novel blue light-emitting naphthalimide derivatives, Dyes Pigments 86 (2010) 190–196.

[13] E.R. Triboni, P. Berci Filho, R.G.S. Berlinck, M.J. Politi, Efficient sonochemical synthesis of 3- and 4-electron withdrawing ring substituted N-Alkyl-1,8-naphthalimides from the related anhydrides, Synth. Commun. 34 (2004) 1989–1999.

[14] J.L. Magalhães, R.V. Pereira, E.R. Triboni, P. Berci Filho, M.H. Gehlen, F.C. Nart, Solvent effect on the photophysical properties of 4-phenoxy-N-methyl-1,8-naphthalimide, J. Photochem. Photobiol. A: Chem. 183 (2006) 165–170.

[15] L. Micaroni, F.C. Nart, I.A. Hümmelgen, Considerations about the electrochemical estimation of the ionization potential of conducting polymers, J. Solid State Electrochem. 7 (2002) 55–59.

[16] R. Reyes, M. Cremona, E.E.S. Teotonio, H.F. Brito, O.L. Malta, Molecular electrophosphorescence in (Sm, Gd)-β-diketonate complex blend for OLED applications, J. Lumin. 134 (2013) 369–373.

[17] I. Grabcheva, C. Petkovb, V. Bojinovc, Infrared spectral characterization of poly(amidoamine) dendrimers peripherally modified with 1,8-naphthalimides, Dyes Pigments 62 (2004) 229–234.

[18] V. Bojinov, I. Grabchev, Synthesis of new polymerizable 1,8-naphthalimide dyes containing a 2-hydroxyphenylbenzotriazole fragment, Dyes Pigments 59 (2003) 277–283.

[19] J. Gawronski, K. Gawronska, P. Skowronek, A. Holmén, 1,8-Naphthalimides as stereochemical probes for chiral amines: a study of electronic transitions and exciton coupling, J. Org. Chem. 64 (1999) 234–241.

[20] C. Coya, R. Blanco, R. Juárez, R. Gómez, R. Martínez, A. Andrés, A.L. Alvarez, C. Zaldo, M.M. Ramos, A. Peña, C. Seoane, J.L. Segura, Synthesis and tunable emission of novel polyfluorene copolymers with 1,8-naphthalimide pendant groups and application in a single layer–single component white emitting device, Europ. Polym. J. 46 (2010) 1778–1789.

[21] T. Chu, O. Song, Hole mobility of N,N′-bis(naphthalen-1-yl)-N,N′-bis(phenyl) benzidine investigated by using space-charge-limited currents, Appl. Phys. Lett. 90 (2007) 2035121–2203513.

[22] V. Coropceanu, J. Cornil, D.S. Filho, Y. Olivier, R. Silbey, J. Bredas, Charge transport in organic semiconductors, Chem. Rev. 107 (2007) 926–952.

[23] J.C. Blakesley, F.A. Castro, W. Kylberg, G.F.A. Dibb, C. Arantes, R. Valaski, M. Cremona, J.S. Kim, J. Kim, Towards reliable charge-mobility benchmark measurements for organic semiconductors, Org. Electron. 15 (2014) 1263–1272.

[24] M.A. Lampert, Simplified theory of space-charge-limited currents in an insulator with traps, Phys. Rev. 103 (1956) 1648–1656.
[25] M. Kiy, P. Losio, I. Baggio, M. Koehler, A. Tappomier, P. Günter, Observation of the Mott–Gurney law in tris (8-hydroxyquinoline) aluminum films, Appl. Phys. Lett. 80 (2002) 1198–1200.
[26] F. Garten, A.R. Schlatmann, R.E. Gill, J. Vrijmoeth, T.M. Klapwijk, G. Hadziioannou, Light emission in reverse bias operation from poly(3-octylthiophene)-based light emitting diodes, Appl. Phys. Lett. 66 (1995) 2540–2542.